

JIAO HUNKUN, O. AVRUNIN

## FEASIBILITY ANALYSIS OF IMPLANT MOVEMENT ALONG ARC TRAJECTORY UNDER NON-CONTACT CONTROL IN MAGNETIC STEREOTAXIC SYSTEM

In this paper, the non-contact control of magnetic implants by changing the external magnetic field in the magnetic stereotaxic system is introduced, and the feasibility of making them move along the arc trajectory is analyzed. Through COMSOL software, the process of moving the miniature magnetic implant along the arc trajectory was simulated, the change of the micro-magnetic implant trajectory after the external magnetic field was changed, the relative position relationship between the large permanent magnets was determined, and the mechanical analysis of the miniature magnetic implant moving along the arc trajectory was carried out. In this experiment, we fix a large permanent magnet, only move the second permanent magnet, first, observe the process of small permanent magnets moving along a straight trajectory, determine the position of the large permanent magnet magnetic field when it contacts the small permanent magnet, and then, analyze the force of the small permanent magnet through the force calculation module, and determine the relative position relationship between the two large permanent magnets by comparing  $F_x$  and  $F_y$ , and when the small permanent magnet will start to move along the arc trajectory. Then, according to the previous data, we move two adjacent large permanent magnets at the same time at a certain interval, record the movement trajectory of the small magnet, Finally, with the force calculation module of the COMSOL software, force analysis of small permanent magnets moving along arc trajectories. The data from this experiment will be used to determine the relative position relationship between two large permanent magnets adjacent to each other during the actual experiment, and under what conditions the small permanent magnets will move along the arc trajectory. The purpose of this experiment is to provide theoretical and data support for the subsequent practical experiments of the magnetic stereotaxic system, and all parameters in the COMSOL software are derived from the actual measurement data, so as to improve the reliability of the simulation results.

**Keywords:** Human health; Magnetic field; COMSOL Software; Permanent magnets; Force analysis.

### Magnetic stereotaxis system

In traditional neurosurgery for brain tissue, craniotomy is usually performed using wire-guided, mechanically controlled surgical instruments with stereotaxic devices [1–5]. The limitation of this method is that the surgical instruments can only move along a straight trajectory, resulting in limited surgical access, great trauma to the tissues around the movement path, and inability to enter the deep structure of brain tissue, which cannot effectively treat brainstem tumors and some extrapyramidal nerve diseases.

Therefore, the magnetic stereotaxic system [6–11] came into being. This method was proposed in 1990 by Howard M. A., Mayburg M., Grady M. S. At present, the method is still in the experimental stage. The magnetic stereotaxic system consists of an external magnetic field, miniature magnetic implants. It works by probing magnetic surgical instruments into the skull, guiding micro-magnetic implants with catheters along pre-designed and calculated trajectories to the lesion via

an external magnetic field, providing hyperthermia to tumors located in deep structures of brain tissue or delivering targeted drugs through catheters. In contrast to traditional neurosurgery, magnetic stereotaxic systems provide non-contact control of miniature magnetic surgical instruments by changing the external magnetic field, and under computer-aided simulation, multiple surgical pathways can be established, allowing the implant to travel along any route to almost any location in the brain. This minimizes the invasiveness of the implant to surrounding tissues during movement. Since the external magnetic field is controlled by the computer according to a pre-designed program and multiple simulations are required before surgery, the difficulty of operation by medical staff is greatly reduced, and the intraoperative safety is greatly improved. These advantages make the magnetic stereotaxic system one of the least invasive methods for surgical intervention against brain tumors, and one of the most promising methods.

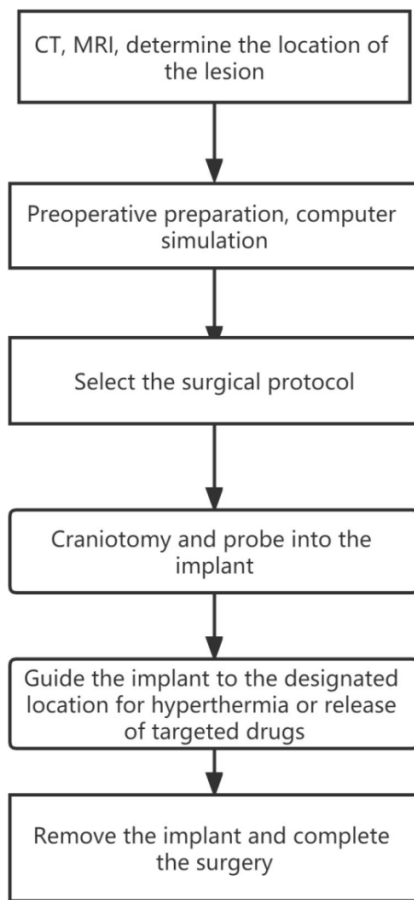


**Fig. 1.** Introduction to the procedure for magnetic stereotactic surgery

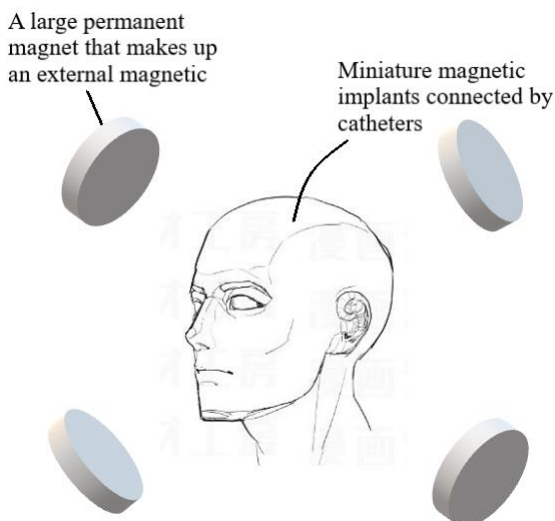


**Fig. 2.** Conceptual diagram of magnetic stereotactic system

In this simulation experiment, the external magnetic field of the magnetic stereotactic system is composed of four large permanent magnets [12, 13], and the small permanent magnets simulate implants. Computer simulation software chooses COMSOL 6.0 [14–16].

## Computer simulation experiments

### Experimental Objective

To control the miniature magnetic implant non-contact by the magnetic stereotactic system to make it move along the arc trajectory.

### Experimental design

Establish a coordinate system in 3D space, small cylindrical permanent magnets are located in the center of the coordinate system, large permanent magnets are set on the  $+X$  and  $+Y$  axes, parameters are set in the simulation software according to the experimental material data, and geometric models are constructed.

#### Simulation experiment parameter settings

(1)  $d_{ion} = 100[\text{mm}] = 0.1[\text{m}]$  (Large permanent magnet diameter);

(2)  $t_{ion} = 10[\text{mm}] = 0.01[\text{m}]$  (Large permanent magnet thickness);

(3)  $d_{NFB} = 1[\text{mm}] = 0.001[\text{m}]$  (Small permanent magnet diameter);

(4)  $l_{NFB} = 2[\text{mm}] = 0.002[\text{m}]$  (Small permanent magnet thickness);

(5) The small permanent magnet boundary is limited to a cylinder with a radius of 0.1 [m] and a height of 0.5 [m];

(6) Large permanent magnets have a maximum distance of 0.41 [m] from the center of 3D space and a closest distance of 0.11 [m], the movable distance of large permanent magnets is 0.3 [m].

### Simulation experiment material property settings

#### Permanent magnets:

(1) Conductivity  $\sigma = 1/1.4[\text{uohm}\times\text{m}][\text{S}/\text{m}]$ ;

(2) Relative permittivity  $\epsilon_r = 1[1]$ ;

(3) Recovery permeability  $\mu_{rec} = 1.02$ ;

(4) Residual flux density norm  $normB_r = 1.3[\text{T}]$ ;

#### air:

(1) Conductivity  $\sigma = 0[\text{uohm}\times\text{m}][\text{S}/\text{m}]$ ;

(2) Relative permittivity  $\epsilon_r = 1[1]$ ;

(3) Recovery permeability  $\mu_{rec} = 1$ .

All the above parameters are theoretical parameters and can be set according to the material parameters required for actual experiments.

Depending on the parameter settings, create a geometric model in 3D space:

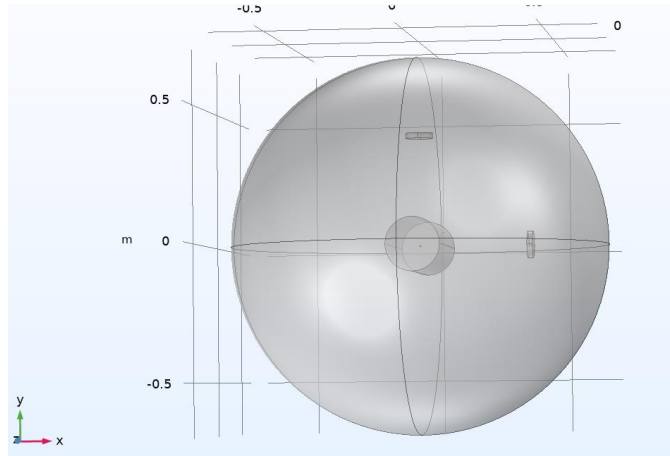


Fig. 3. Geometric models based on parameters in COMSOL software

### Equations and formulas for simulation experiments

In this simulation experiment, the external magnetic field of the magnetic stereoscopic positioning system is composed of large permanent magnets, and the magnetic field of the permanent magnets is a static magnetic field. Therefore, "magnetic field, no current (MFNC)" was selected in the COMSOL physics.

In the constitutive relations  $B-H$ , the magnetization model [17] needs to introduce the magnetization vector field  $M$ , and the magnetic field strength  $H$ , which are expressed as:

$$H = \frac{B}{\mu_0} - M \quad (1)$$

or:

$$B = \mu_0 (H + M), \quad (2)$$

where  $\mu_0$  – is the magnetic permeability;

$B$  is Magnetic flux density.

The remaining flux density is then selected in the magnetization model with the following expression:

$$B = \mu_0 \mu_{rec} H + B_r ; \quad (3)$$

$$B_r = \|B_r\| \frac{e}{\|e\|}, \quad (4)$$

where  $B$  is the magnetic flux density;  $\mu_0$  is the vacuum permeability;  $\mu_{rec}$  is recoil permeability;  $B_r$  is residual flux density;  $\|B_r\|$  is residual flux density norm;  $e$  is residual flux direction.

### Simulation results

The large permanent magnet located on the  $+X$  axis begins to move towards the center position. When the first large permanent magnet is 0.36 [m] from the center position, its magnetic field gradually touches the small permanent magnet.

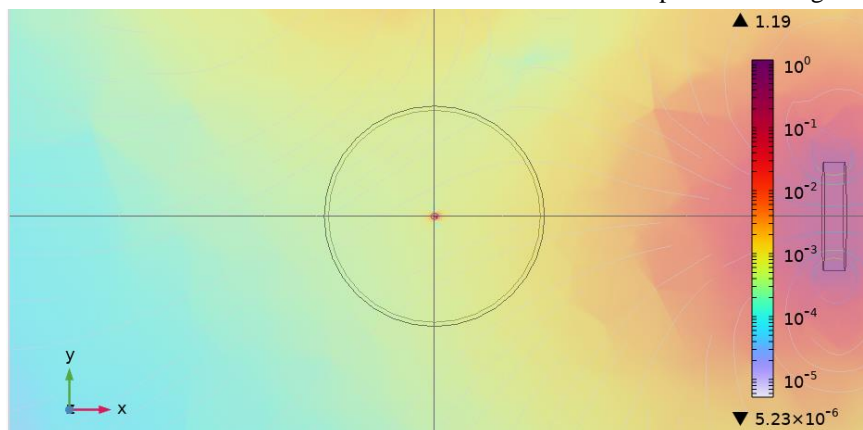
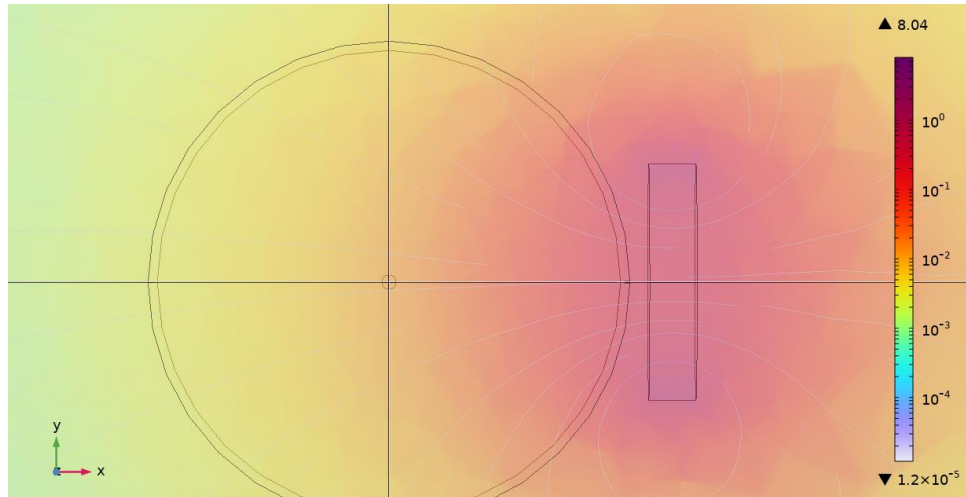


Fig. 4. The magnetic field of a large permanent magnet gradually touches the small permanent magnet

When its magnetic field touches a small permanent magnet, the small permanent magnet begins to approach the first large permanent magnet.

When the small permanent magnet moves to the boundary position, it is blocked by the boundary and stays on the boundary.



**Fig. 5.** Small permanent magnets are blocked by the boundary and stay on the boundary

The first large permanent magnet began to move away, and the second large permanent magnet gradually approached, at this time, the magnetic field lines around the small permanent magnet could be clearly seen, but the same simulation software could not intuitively see that the magnetic field of the second large permanent magnet touched the small permanent magnet.

To study the movement of small permanent magnets along arc trajectories under non-contact control, therefore, we use the "Force Calculation" module included in the software to analyze the force of small

permanent magnets located at boundary locations. The distance between the first large permanent magnet and the center is  $dis\_ion$ , the distance of the second large permanent magnet from the center is  $dis\_ion1$ ,  $F_x$  is the  $X$ -axis component of the force experienced by the small permanent magnet, and  $F_y$  is the on- $Y$ -axis component of the force experienced by the small permanent magnet.

First, let's assume that the first large permanent magnet stays 0.22 [m] from the center and only the second large permanent magnet is running.

**Table 1.** Force analysis of a small permanent magnet at the boundary position when the position of the first large permanent magnet remains unchanged and the second large permanent magnet gradually approaches the center position

$dis\_ion$ [m]	$dis\_ion1$ [m]	$F_x$ [N]	$F_y$ [N]
0.22	0.24	$7.199 \times 10^{-9}$	$5.408 \times 10^{-9}$
0.22	0.23	$7.916 \times 10^{-9}$	$6.877 \times 10^{-9}$
0.22	0.22	$8.715 \times 10^{-9}$	$8.561 \times 10^{-9}$
0.22	0.21	$9.883 \times 10^{-9}$	$11.541 \times 10^{-9}$
0.22	0.20	$11.180 \times 10^{-9}$	$15.123 \times 10^{-9}$
0.22	0.19	$12.598 \times 10^{-9}$	$19.332 \times 10^{-9}$
0.22	0.18	$14.321 \times 10^{-9}$	$26.112 \times 10^{-9}$

From the above table, we find that when the distance from the second large permanent magnet to the center position is less than the distance from the first large permanent magnet to the center position, the  $Y$ -axis component of the force of the small

permanent magnet is greater than the  $X$ -axis component. That is, when  $dis\_ion1 < dis\_ion$ ,  $F_y > F_x$ . To verify this result, we set the first large permanent magnet to be located 0.18 [m] from the center and re-analyzed the force on the small permanent magnet.

**Table 2.** Force analysis of a small permanent magnet when the first large permanent magnet is 0.18 [m] from the center

$dis\_ion$ [m]	$dis\_ion1$ [m]	$F_x$ [N]	$F_y$ [N]
0.18	0.21	$22.726 \times 10^{-9}$	$13.959 \times 10^{-9}$
0.18	0.20	$24.941 \times 10^{-9}$	$17.814 \times 10^{-9}$
0.18	0.19	$27.614 \times 10^{-9}$	$23.142 \times 10^{-9}$
0.18	0.18	$31.381 \times 10^{-9}$	$31.143 \times 10^{-9}$
0.18	0.17	$35.683 \times 10^{-9}$	$41.613 \times 10^{-9}$
0.18	0.16	$40.918 \times 10^{-9}$	$56.554 \times 10^{-9}$
0.18	0.15	$48.237 \times 10^{-9}$	$81.361 \times 10^{-9}$

According to Table 1 and Table 2, we can clearly see that when the distance from the first large permanent magnet to the center position is greater than the distance from the second large permanent magnet to the center position, the force on the  $Y$  axis of the small permanent magnet is greater than the component force on the  $X$  axis, that is, when  $dis\_ion1 < dis\_ion$ ,  $F_x < F_y$ . In order to facilitate practical experiments, we set the distance from the first large permanent magnet to the center position and the distance from the second large permanent magnet to the center position to be 0.05 [m], that is, when the first large permanent magnet begins to move 0.05 [m] to the center position, the second large permanent magnet begins to approach the center

position, and the two large permanent magnets move at the same speed.

During the movement of the two large permanent magnets, we perform a force analysis on the small permanent magnets again. In order to determine the position of the two large permanent magnets when the small permanent magnet initially moves, the position of the small permanent magnet does not change during the analysis, and always stays at the boundary position. It can be determined that when the first large permanent magnet is closest to the center, the small permanent magnet is affected by its magnetic field and stays at the boundary position on the  $+X$  axis, so the initial positions of the two large permanent magnets are  $dis\_ion = 0.11$  [m],  $dis\_ion1 = 0.16$  [m], respectively.

**Table 3.** Two large permanent magnets operate at the same time, and the force analysis of small permanent magnets

$dis\_ion$ [m]	$dis\_ion1$ [m]	$F_x$ [N]	$F_y$ [N]
0.11	0.16	$443.82 \times 10^{-9}$	$97.217 \times 10^{-9}$
0.12	0.15	$234.78 \times 10^{-9}$	$120.96 \times 10^{-9}$
0.13	0.14	$188.50 \times 10^{-9}$	$148.66 \times 10^{-9}$
0.14	0.13	$167.14 \times 10^{-9}$	$202.43 \times 10^{-9}$
0.15	0.12	$157.48 \times 10^{-9}$	$289.53 \times 10^{-9}$
0.16	0.11	$152.98 \times 10^{-9}$	$442.38 \times 10^{-9}$
0.17	0.12	$100.73 \times 10^{-9}$	$270.51 \times 10^{-9}$
0.18	0.13	$67.94 \times 10^{-9}$	$176.42 \times 10^{-9}$
0.19	0.14	$46.69 \times 10^{-9}$	$115.81 \times 10^{-9}$
0.20	0.15	$32.37 \times 10^{-9}$	$75.34 \times 10^{-9}$
0.21	0.16	$22.83 \times 10^{-9}$	$52.09 \times 10^{-9}$

It can be clearly seen from Table 3 that when the first large permanent magnet begins to gradually move away, the second large permanent magnet gradually approaches,  $F_x$  gradually decreases,  $F_y$  gradually increases, when the second large permanent magnet moves 0.11 [m] from the center position,  $F_y$  reaches the maximum, and then the second large permanent magnet begins to gradually move away and  $F_y$  gradually

decreases. Thus, when the distance from the second large permanent magnet to the center position is less than the distance from the first large permanent magnet to the central position, that is, when  $dis\_ion1 < dis\_ion$ ,  $F_x < F_y$ , at which point the small permanent magnet begins to move along the boundary towards the second large permanent magnet.

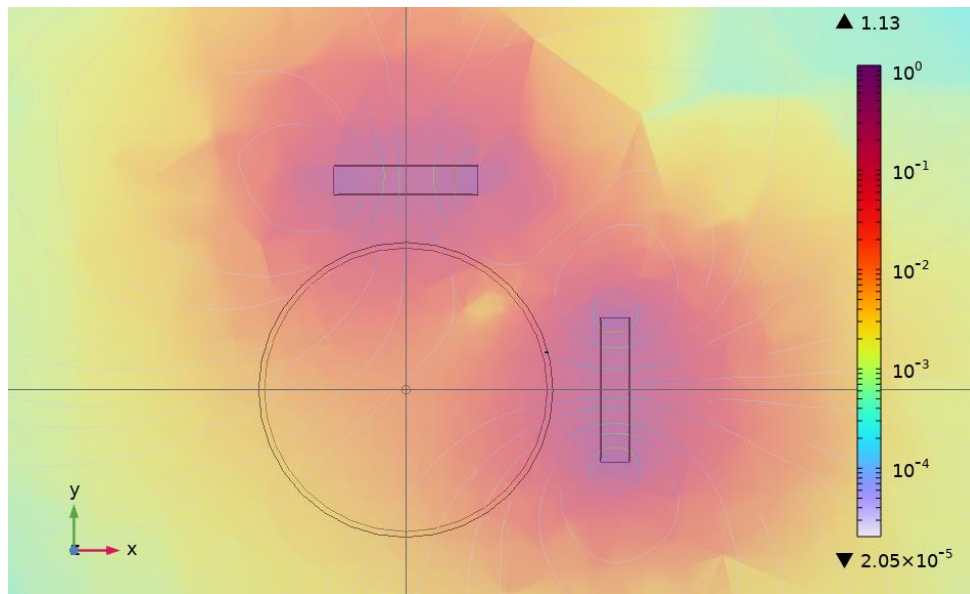


**Fig. 6.** The small permanent magnet begins to move along the boundary towards the second large permanent magnet

The closer to the second large permanent magnet, the greater the influence of its magnetic field on the small permanent magnet, that is, the greater the  $F_y$ , but at this time the small permanent magnet is still affected by the magnetic field of the first large permanent magnet, that is,  $F_x$  gradually decreases, which makes the small permanent magnet move along the boundary to the second large permanent magnet.

The small permanent magnet is captured by the magnetic field of the second large permanent magnet and stays on the boundary of the  $+Y$  axis. That is, when the second large permanent magnet is closest to the center, i.e.,  $dis\_ion1 = 0.11[m]$ , the small permanent magnet has moved to the boundary position along the arc trajectory.

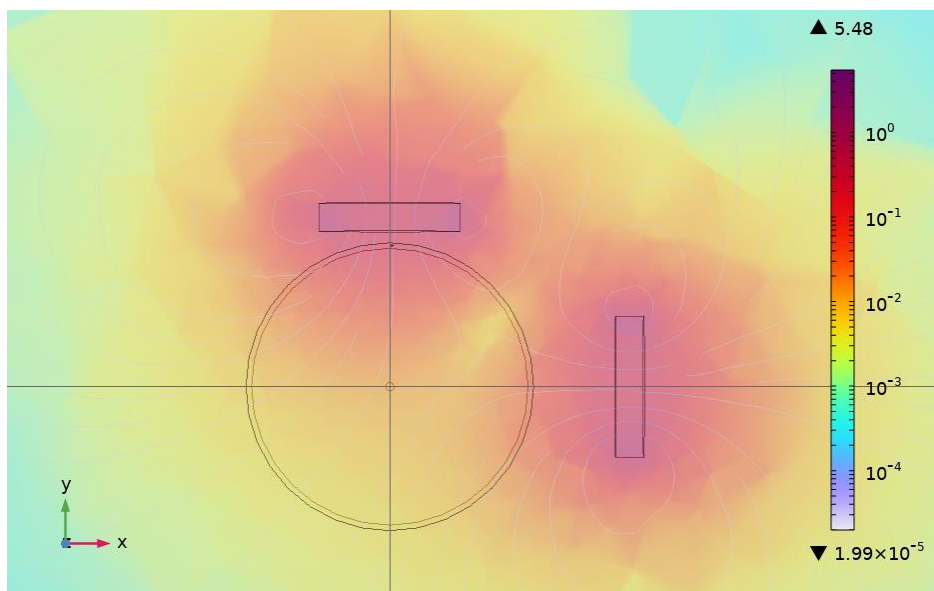


**Fig. 7.** The small permanent magnet reaches the end of the arc trajectory

As the two large permanent magnets move away, the small permanent magnets remain at the boundary position.

In order to determine the average velocity of a small permanent magnet moving along an arc trajectory towards a second large permanent magnet, we need

to perform a force analysis on the movement of the small permanent magnet.  $n$  is the angle of the arc

trajectory of the small permanent magnet moving along the boundary.

**Table 4.** Force analysis during the movement of small permanent magnets

$dis\_ion$ [m]	$dis\_ion1$ [m]	$n$	$F_x$ [N]	$F_y$ [N]
0.130	0.140	0	$188.50 \times 10^{-9}$	$148.66 \times 10^{-9}$
0.135	0.135	15	$176.37 \times 10^{-9}$	$172.81 \times 10^{-9}$
0.140	0.130	30	$167.14 \times 10^{-9}$	$202.43 \times 10^{-9}$
0.145	0.125	45	$159.59 \times 10^{-9}$	$236.59 \times 10^{-9}$
0.150	0.120	60	$157.48 \times 10^{-9}$	$289.53 \times 10^{-9}$
0.155	0.115	75	$155.41 \times 10^{-9}$	$353.71 \times 10^{-9}$
0.160	0.110	90	$152.98 \times 10^{-9}$	$442.38 \times 10^{-9}$

In order to intuitively see the force change of the small permanent magnet during the moving process, according to the above table, we draw

a line diagram of the two component forces  $F_x$  and  $F_y$  of the small permanent magnet during the moving process.

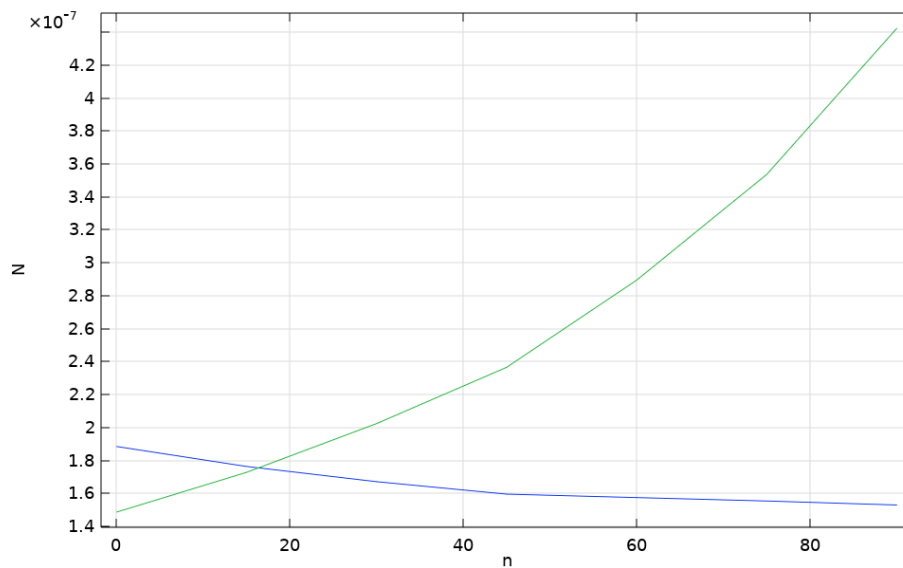


**Fig. 8.** Force analysis of small permanent magnets as they move along an arc trajectory

### Simulation experiment conclusion

Through the above simulation experiments, we find that in the process of moving the small permanent magnet to the second large permanent magnet, as the  $F_y$  gradually increases,  $F_x$  gradually decreases, and the force direction of the small permanent magnet gradually points to the  $Y$  axis direction, therefore, the small permanent magnet moves along the boundary towards the second large permanent magnet, and the trajectory is an arc. According to Tables 1–3, we find that when the distance of the second large permanent

magnet from the center position is less than the distance of the first large permanent magnet from the center, that is, at  $dis\_ion1 < dis\_ion$ , the direction of the magnetic field around the small permanent magnet located at the boundary position of the  $X$ -axis changes, the  $F_y$  increases, and the small permanent magnet begins to move towards the second large permanent magnet. Through Table 4, we calculate the changes of  $F_x$  and  $F_y$  during the movement of small permanent magnets along the boundary when the  $dis\_ion$  and  $dis\_ion1$  differ by 0.05 [m], and determine the relative positions of

the two large permanent magnets for subsequent practical experiments.

Through the simulation experiment of COMSOL software, we can clearly observe that by changing the external magnetic field, under non-contact control,

small permanent magnets can move along an arc trajectory. This shows that it is feasible to non-contact control the implant to move along the arc trajectory in the magnetic stereotaxic system, and at the same time provides a theoretical basis for subsequent experiments.

## References

1. Kall, B A. (1987), "The impact of computer and imaging technology on stereotactic surgery". *Stereotactic and Functional Neurosurgery*. No. 50(1–6): 9–22. DOI: 10.1159/000100676
2. Avrunin, O., Tymkovich, M., Semenets, V., & Piatyokop, V. (2019), "Computed tomography dataset analysis for stereotaxic neurosurgery navigation". *Paper presented at the Proceedings of the International Conference on Advanced Optoelectronics and Lasers, CAOL*. P. 606–609. DOI:10.1109/CAOL46282.2019.9019459
3. Avrunin, O. G., Alkhorayef, M., Saied, H. F. I., & Tymkovich, M. Y. (2015), "The surgical navigation system with optical position determination technology and sources of errors". *Journal of Medical Imaging and Health Informatics*. No. 5(4), P. 689–696. DOI:10.1166/jmihi.2015.1444
4. Avrunin, O. G., Tymkovich, M. Y., Moskovko, S. P., Romanyuk, S. O., Kotyra, A., & Smailova, S. (2017), "Using a priori data for segmentation anatomical structures of the brain". *Przegląd Elektrotechniczny*. No. 93(5), P. 104–107. DOI:10.15199/48.2017.05.20
5. Chen, Y, Godage, I, Su, H. et al. (2019), "Stereotactic systems for MRI-guided neurosurgeries: a state-of-the-art review". *Annals of biomedical engineering*, No. 47(1–4). P. 335–353.
6. Hunkun, Jiao, Avrunin, O. (2023), "Explore the feasibility study of magnetic stereotaxic system". *Optoelectronic Information-Power Technologies*, No. 45(1). P. 86-96. DOI:10.31649/1681-7893-2023-45-1-86-96
7. Grady, S M, Howard, III M A, Broaddus, W C, et al. "Magnetic stereotaxis: a technique to deliver stereotactic hyperthermia". *Neurosurgery*, 1990, No. 27(6). P. 1010–1016. available at: <https://pubmed.ncbi.nlm.nih.gov/2274121/>
8. Nelson, B. J., Gervasoni, S., Chiu, P. W. Y., et al.(2022), "Magnetically actuated medical robots: An in vivo perspective". *Proceedings of the IEEE*. No. 110(7). P. 1028–1037. DOI:10.1109/JPROC.2022.3165713
9. Grady, M. S., Howard, M. A., Dacey, R. G., et al.(2000), "Experimental study of the magnetic stereotaxis system for catheter manipulation within the brain". *Journal of neurosurgery*. No. 93(2). P. 282–288. DOI: 10.3171/jns.2000.93.2.0282
10. Hunkun, J., Avrunin, O. (2022), "Possibilities of Field Formation by Permanent Magnets in Magnetic Stereotactic Systems", *IEEE 3rd KhPI Week on Advanced Technology (KhPIWeek)*, Kharkiv, Ukraine. P. 1–4. DOI: 10.1109/KhPIWeek57572.2022.9916450
11. Coey, J. M. D. (2002), "Permanent magnet applications". *Journal of Magnetism and Magnetic Materials*. No. 248(3). P. 441–456. DOI: 10.1016/S0304-8853(02)00335-9
12. Calin, M. D., Helerea, E. "Temperature influence on magnetic characteristics of NdFeB permanent magnets". *7th international symposium on advanced topics in electrical engineering (ATEE)*. IEEE, 2011. P. 1–6. available at: [https://www.researchgate.net/publication/241186295\\_Temperature\\_influence\\_on\\_magnetic\\_characteristics\\_of\\_NdFeB\\_permanent\\_magnets](https://www.researchgate.net/publication/241186295_Temperature_influence_on_magnetic_characteristics_of_NdFeB_permanent_magnets)
13. Pepper, D W, Heinrich, J C. "The finite element method: basic concepts and applications with MATLAB, MAPLE, COMSOL". CRC press. 2017. 628 p. available at: <https://handoutset.com/wp-content/uploads/2022/05/The-finite-element-method-basic-concepts-and-applications-with-MATLAB-MAPLE-and-COMSOL-Heinrich-Juan-C.-Pepper-Darrell-W.pdf>
14. Pryor, R W. "Multiphysics modeling using COMSOL: a first principles approach". Jones & Bartlett Publishers, 2009. 871 p. available at: <http://dl.poweren.ir/downloads/PowerEn/Book/2019/Mar/%DA%A9%D8%AA%D8%A7%D8%A8%20%D8%A2%D9%85%D9%88%D8%B2%D8%B4%20%D8%AC%D8%A7%D9%85%D8%B9%20%DA%A9%D8%A7%D9%85%D8%B3%D9%88%D9%84%20%28PowerEn.ir%29.pdf>
15. Chen, W X, Wu, J Y. (2022), "Phase-field cohesive zone modeling of multi-physical fracture in solids and the open-source implementation in Comsol Multiphysics[J]. *Theoretical and Applied Fracture Mechanics*, No. 117. P. 103153. DOI: 10.1016/j.tafmec.2021.103153
16. Zhang, Y, Leng, Y, Zhang, H, et al. "Comparative study on equivalent models calculating magnetic force between permanent magnets". *Journal of Intelligent Manufacturing and Special Equipment*, 2020, No. 1(1). P. 43–65. available at: <https://www.emerald.com/insight/content/doi/10.1108/JIMSE-09-2020-0009/full/html>

**Цзяо Ханкунь** – Харківський національний університет радіоелектроніки, аспірант кафедри біомедичної інженерії, Харків, Україна; e-mail: 1350829683@qq.com, jiao.hankun@nure.ua. ORCID ID: <https://orcid.org/0000-0003-0992-5344>

**Аврунін Олег Григорович** – доктор технічних наук, професор, Харківський національний університет радіоелектроніки, завідувач кафедри біомедичної інженерії, Харків, Україна; e-mail: oleh.avrunin@nure.ua; ORCID ID: <https://orcid.org/0000-0002-6312-687X>

**Jiao Hunkun** – Kharkiv National University of Radio Electronics, PhD student at the Department of Biomedical Engineering, Kharkiv, Ukraine.

**Avrunin Oleg** – Doctor of Sciences (Engineering), Professor, Kharkiv National University of Radio Electronics, Head of the Department of Biomedical Engineering, Kharkiv, Ukraine.

## АНАЛІЗ МОЖЛИВОСТІ ПЕРЕМІЩЕННЯ ІМПЛАНТУ ПО ДУГОВІЙ ТРАЄКТОРІЇ ПІД БЕЗКОНТАКТНИМ КОНТРОЛЕМ У МАГНІТНІЙ СТЕРЕОТАКСИЧНІЙ СИСТЕМІ

У статті подано безконтактне керування магнітними імплантами способом зміни зовнішнього магнітного поля в магнітній стереотаксичній системі та проаналізовано можливість їх переміщення по дуговій траєкторії. За допомогою програмного забезпечення COMSOL змодельовано процес переміщення мініатюрного магнітного імпланту по дуговій траєкторії, досліджено зміну траєкторії мікромагнітного імпланту після зміни зовнішнього магнітного поля, визначено взаємне розташування великих постійних магнітів та проведено механічний аналіз переміщення мініатюрного магнітного імпланту по дуговій траєкторії. У цьому експерименті ми фіксуємо великий постійний магніт, рухаємо лише другий постійний магніт, спочатку спостерігаємо процес руху малих постійних магнітів по прямій траєкторії, визначаємо положення магнітного поля великого постійного магніту, коли він контактує з малим постійним магнітом, а потім аналізуємо силу малого постійного магніту за допомогою модуля розрахунку сили та встановлюємо відносне положення між двома великими постійними магнітами, порівнюючи  $F_x$  та  $F_y$ , і коли малий постійний магніт почне рухатись по дуговій траєкторії. Далі, згідно з попередніми результатами, ми переміщуємо два сусідні великі постійні магніти одночасно з певним інтервалом, записуємо траєкторію руху малого магніту, і, нарешті, за допомогою модуля розрахунку сил програмного забезпечення COMSOL здійснюємо силовий аналіз руху малих постійних магнітів по дугових траєкторіях. Результати проведеного експерименту будуть використані для визначення взаємного розташування двох великих постійних магнітів, розташованих поруч під час дослідження, для з'ясування того, за яких умов малі постійні магніти будуть рухатися по дуговій траєкторії. Метою цього експерименту є забезпечення теоретичної та інформаційної підтримки для подальших практичних досліджень магнітної стереотаксичної системи, коли всі параметри в програмному забезпеченні COMSOL отримані на основі фактичних показників вимірювань для підвищення вірогідності результатів симуляції.

**Ключові слова:** здоров'я людини; магнітне поле; програмне забезпечення COMSOL; постійні магніти; силовий аналіз.

### Бібліографічні описи / Bibliographic descriptions

Цзяо Ханкунь, Аврунін О. Г. Аналіз можливості переміщення імпланту по дуговій траєкторії під безконтактним контролем у магнітній стереотаксичній системі. *Сучасний стан наукових досліджень та технологій в промисловості*. 2023. № 3 (25). С. 174–182. DOI: <https://doi.org/10.30837/ITSSI.2023.25.174>

Hunkun, J., Avrunin, O. (2023), "Feasibility analysis of implant movement along arc trajectory under non-contact control in magnetic stereotaxic system", *Innovative Technologies and Scientific Solutions for Industries*, No. 3 (25), P. 174–182. DOI: <https://doi.org/10.30837/ITSSI.2023.25.174>